

High-power IGBT Modules for Industrial Use

Takashi Nishimura
Hideaki Kakiki
Takatoshi Kobayashi

1. Introduction

Power devices used in industrial-use high capacity inverter system applications are predominately GTO (gate turnoff) thyristors, which easily handle high voltages and currents. However, recent advances in high-voltage and high-power technology for IGBT (insulated gate bipolar transistor) modules have been remarkable, and IGBT modules are being used nowadays in applications that had previously required the use of GTO thyristors. IGBT modules have an insulated module structure that differs from the pressure contact structure of a GTO thyristor and that facilitates assembly, use and maintenance, and as a result, the field of IGBT module applications is expanding exponentially.

In response to the diversifying needs of recent years, Fuji Electric has been actively developing products for the recently growing market of high-power applications.

Targeting high-power industrial-use applications, Fuji Electric has equipped its U4-series of chips (hereafter referred to as U4-chips), an improved version of its U-series of chips (hereafter referred to as U-chips), with a copper base to develop high-power IGBT modules having current capacities of 1,600 A for a 130 × 140 (mm) (1-in-1 and 2-in-1) package and 3,600 A for a 190 × 140 (mm) (1-in-1) package, and high-voltage ratings of 1,200 V and 1,700 V. This paper introduces the summary and technical development of the modules.

2. Product Lineup

Table 1 shows Fuji Electric's product lineup of high-power IGBT modules. The module lineup consists of 1,200 V and 1,700 V voltage classes, three types of packages, and current ratings of 600 to 3,600 A among a total of 14 types of products. Figure 1 shows an external view of the packages.

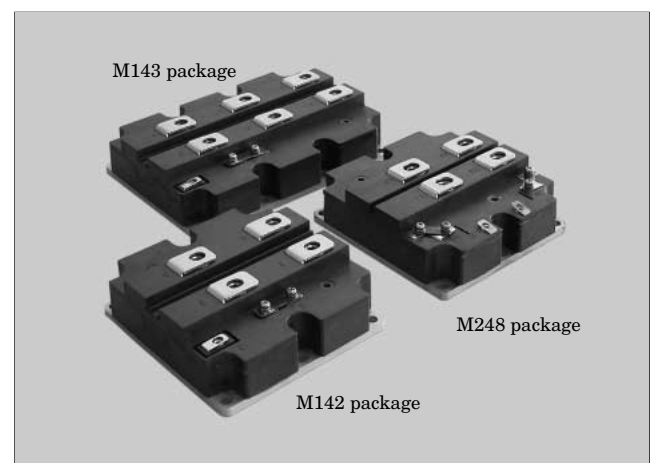
3. Electrical Characteristics

Electrical characteristics of modules that use U4-

Table 1 Fuji Electric's product lineup of high-power IGBT modules

	Model number	Rated voltage (V)	Rated current (A)	Package size (mm)	Package type
1 in 1	1MBI1200U4C-120	1,200	1,200	130 × 140 × 38	M142
	1MBI1600U4C-120		1,600		
	1MBI2400U4D-120		2,400	190 × 140 × 38	M143
	1MBI3600U4D-120		3,600		
	1MBI1200U4C-170	1,700	1,200	130 × 140 × 38	M142
	1MBI1600U4C-170		1,600		
	1MBI2400U4D-170		2,400	190 × 140 × 38	M143
	1MBI3600U4D-170		3,600		
2 in 1	2MBI600U4G-120	1,200	600	130 × 140 × 38	M248
	2MBI800U4G-120		800		
	2MBI1200U4G-120		1,200		
	2MBI600U4G-170	1,700	600		
	2MBI800U4G-170		800		
	2MBI1200U4G-170		1,200		

Fig.1 External view of Fuji Electric's high-power IGBT modules



chips are described below in comparison to modules that use U-chips, and the 2MBI1200U4G-170 (2-in-1 1,200 A/1,700 V) is presented at the representative model.

3.1 Absolute maximum ratings and electrical characteristics

Table 2 lists the absolute maximum ratings and

Table 2 Maximum ratings and electrical characteristics (model No.: 2MB1200U4G-170)

(a) Maximum ratings ($T_j = T_c = 25^\circ\text{C}$, unless otherwise specified)

Item	Symbol	Condition	Maximum rating	Unit	
Collector – emitter voltage	V_{CES}	$V_{GE} = 0\text{ V}$	1,700	V	
Gate – emitter voltage	V_{GES}	–	± 20	V	
Collector current	$I_{C(DC)}$	Continuous	$T_c = 80^\circ\text{C}$	1,200	A
		$I_{C(pulse)}$	1 ms	$T_c = 80^\circ\text{C}$	2,400
Max. power dissipation	P_C	1 device	4,960	W	
Max. junction temperature	$T_{j\max}$	–	150	$^\circ\text{C}$	
Storage temperature	T_{stg}	–	-40 to +125	$^\circ\text{C}$	
Isolation voltage	V_{iso}	AC : 1 ms	3,400	V	

(b) Electrical characteristics

($T_j = T_c = 25^\circ\text{C}$, unless otherwise specified)

Item	Symbol	Test condition	Min.	Typ.	Max.	Unit	
Zero gate voltage collector current	I_{CES}	$V_{GE} = 0\text{ V}$ $T_j = 125^\circ\text{C}$ $V_{CE} = 1,700\text{ V}$	–	–	1.0	mA	
Gate – emitter leakage current	I_{GES}	$V_{GE} = \pm 20\text{ V}$	–	–	1.6	μA	
Gate – emitter threshold voltage	$V_{GE(th)}$	$V_{CE} = 20\text{ V}$ $I_C = 1.2\text{ A}$	5.5	6.5	7.5	V	
Collector – emitter saturation voltage (sense terminal)	$V_{CE(sat)}$	$V_{GE} = +15\text{ V}$ $I_C = 1,200\text{ A}$	$T_j = 25^\circ\text{C}$	–	2.25	–	V
			$T_j = 125^\circ\text{C}$	–	2.65	–	
Input capacitance	C_{ies}	$V_{GE} = 0\text{ V}$ $V_{CE} = 10\text{ V}$ $f = 1\text{ MHz}$	–	110	–	nF	
Turn-on time	t_{on}	$V_{CC} = 900\text{ V}$ $I_C = 1,200\text{ A}$ $V_{GE} = \pm 15\text{ V}$ $R_G = +4.7/-1.2\ \Omega$ $T_j = 125^\circ\text{C}$	–	3.10	–	μs	
	t_r		–	1.25	–		
Turn-off time	t_{off}		–	1.45	–	μs	
	t_f		–	0.25	–		
Forward on-voltage (sense terminal)	V_F	$V_{GE} = 0\text{ V}$ $I_F = 1,200\text{ A}$	$T_j = 25^\circ\text{C}$	–	1.80	–	V
			$T_j = 125^\circ\text{C}$	–	2.00	–	
Reverse recovery time	t_{rr}	$V_{CC} = 900\text{ V}$ $I_F = 1,200\text{ A}$ $T_j = 125^\circ\text{C}$	–	0.45	–	μs	

(c) Thermal characteristics

Item	Symbol	Condition	Min.	Typ.	Max.	Unit
Thermal resistance (for 1 device)	$R_{th(j-c)}$	IGBT	–	–	0.0252	K/W
		FWD	–	–	0.042	

electrical characteristics.

3.2 V-I characteristics

Figure 2 shows the $V_{CE(sat)}-I_C$ characteristics and Fig. 3 shows the V_F-I_F characteristics. The saturation voltage of the IGBT chip was designed to decrease the injection efficiency of the pnp transistor, and without applying lifetime control, to increase the transport efficiency and provide a positive temperature coefficient. Moreover, by optimizing lifetime control of the FWD (free wheeling diode) chip, the forward on-voltage is provided with a positive temperature coefficient as in the IGBT, and this is advantageous for parallel connections to both the IGBT chip and the FWD chip.

3.3 Switching characteristics

(1) Turn-on characteristic

Modules that use the U4-chip employ a new structure in order to optimize the balance between input capacitance (C_{ies}) and reverse transfer capacitance (C_{res}), and as a result, their turn-on loss is drastically reduced. Figure 4 shows turn-on waveforms for an inductive load under the conditions of $V_{CC} = 900\text{ V}$, $I_C = 1,200\text{ A}$, $R_{gon} = 1.8\ \Omega$ and $T_j = 125^\circ\text{C}$. When driven with the same gate resistance (R_{gon}), the module that used the U4-chip (U4-module) had a smaller tail voltage and approximately 50 % less turn-on loss (E_{on}) than the module that used the U-chip (U-

Fig.2 $V_{CE(sat)}-I_C$ characteristics

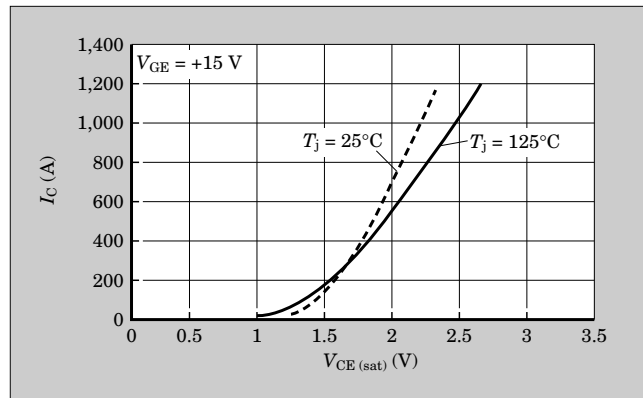


Fig.3 V_F-I_F characteristics

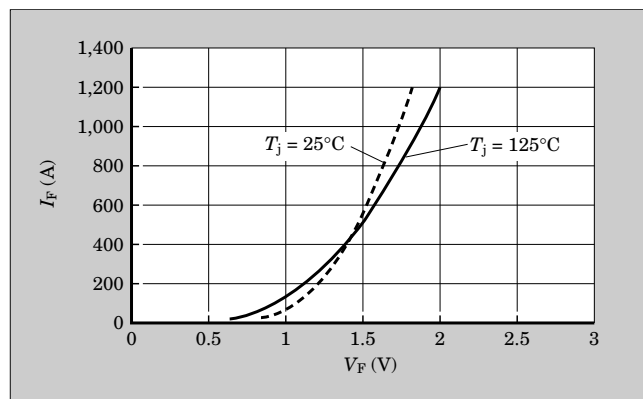


Fig.4 Turn-on waveforms ($V_{CC} = 900 \text{ V}$, $I_C = 1,200 \text{ A}$, 125°C)

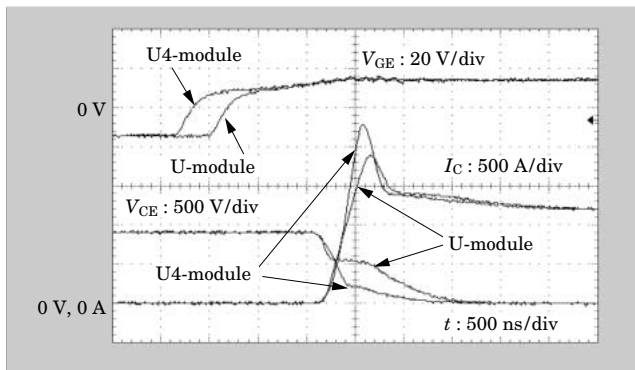


Fig.5 Turn-off waveforms ($V_{CC} = 900 \text{ V}$, $I_C = 1,200 \text{ A}$, 125°C)

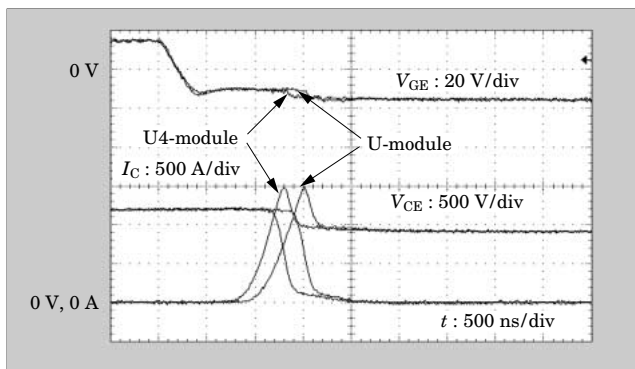
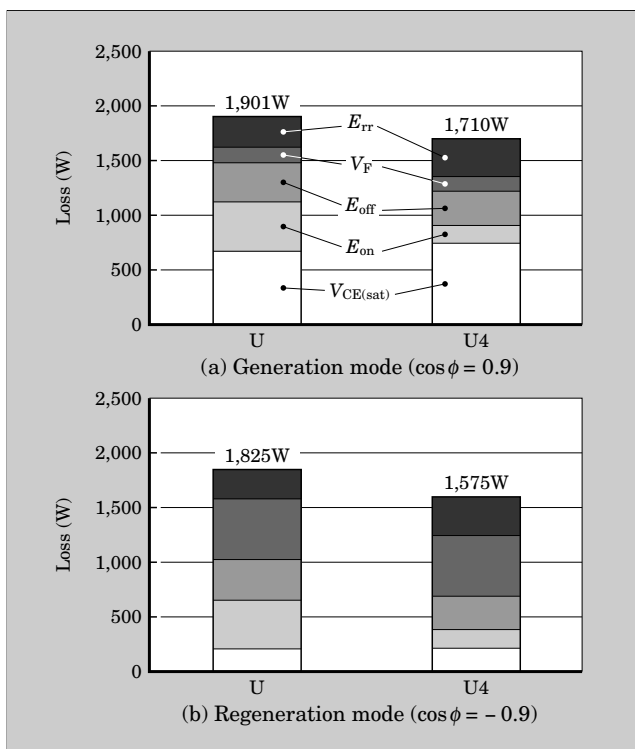


Fig.6 PWM inverter power loss simulation



module).

(2) Turn-off characteristic

Figure 5 shows turn-off waveforms for an inductive load under the conditions of $V_{CC} = 900 \text{ V}$, $I_C = 1,200 \text{ A}$,

Fig.7 Low-current reverse recovery characteristics

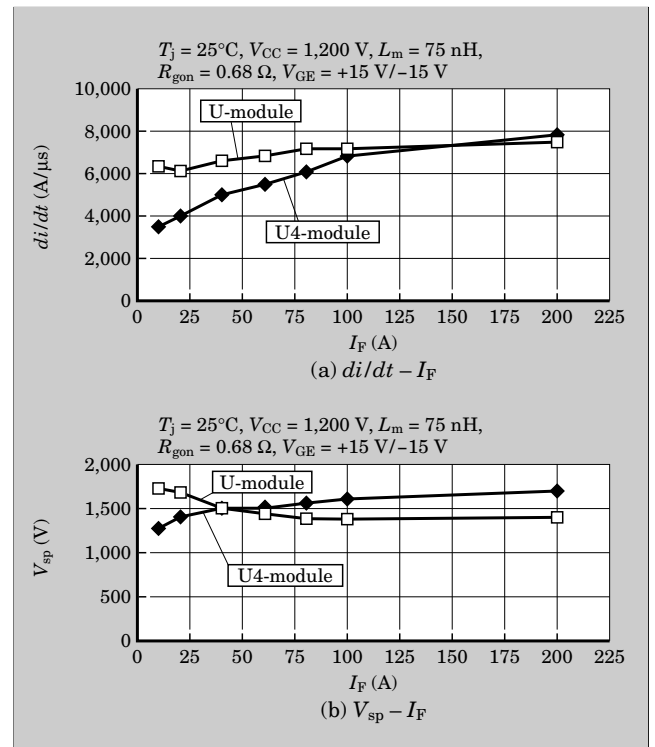
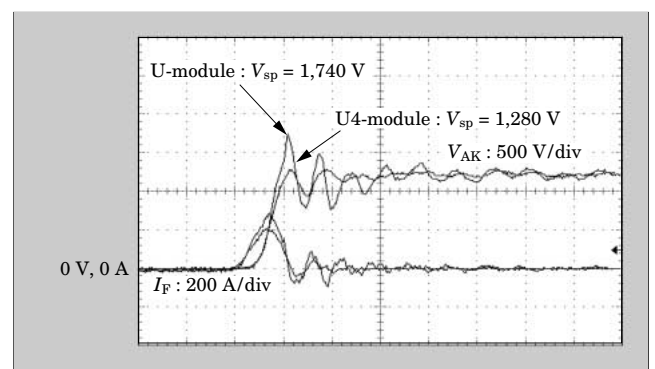


Fig.8 Low-current reverse recovery waveforms ($V_{AK} = 1,200 \text{ V}$, $I_F = 10 \text{ A}$, 25°C)



$R_{goff} = 1.2 \Omega$ and $T_j = 125^\circ\text{C}$. When driven with the same gate resistance (R_{goff}), the turn-off loss was approximately 5 % lower for the U4-module than for the U-module.

(3) PWM inverter power loss simulation

Figure 6 shows the results of a simulation of inverter power loss when operated under the same conditions ($I_{out} = 860 \text{ A}_{rms}$, $\cos \phi = 0.9$ and -0.9 , $f_c = 2.5 \text{ kHz}$). The power loss generated in the U4-module was approximately 10 % less during generation mode and approximately 14 % less during regeneration mode than that of the U-module.

(4) Low-current reverse recovery characteristics

The characteristic features of U4-modules, reduced low-current turn-on di/dt and improved gate resistance controllability of the turn-on di/dt , enable suppression of the surge voltage at the event of reverse

recovery. Figure 7 shows the low-current reverse recovery characteristics. It can be seen that the low-current turn-on di/dt is smaller and that surge voltage is suppressed to a greater extent for the U4-module in comparison to the U-module. Figure 8 shows waveforms obtained under the conditions of $V_{AK} = 1,200 \text{ V}$, $I_F = 10 \text{ A}$, and $R_{gon} = 0.68 \Omega$. From this figure and from Fig. 7(b), it can be seen that the surge voltage is decreased from 1,740 V to 1,280 V.

4. Package Technology for High-power IGBT Modules

High capacity inverter systems require high reliability, and ensuring the reliability of the power devices used to construct such systems is extremely important. To realize power devices with greater capacity, it is necessary that many chips be connected in parallel inside a module, and it is important that the current balance and generation of heat are maintained with an equal distribution.

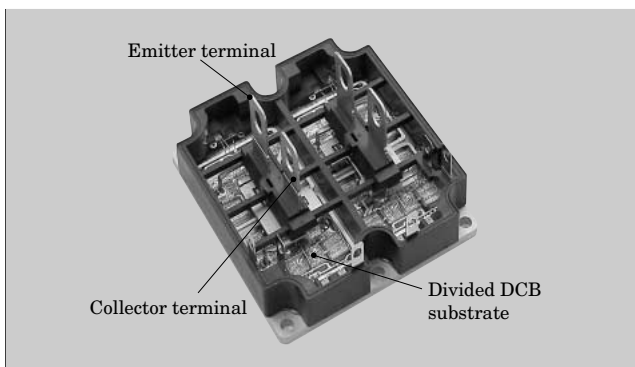
4.1 Chip characteristics

As described in paragraph 3.2, high-power IGBT modules are equipped with chips having a positive temperature coefficient. In chips having a positive temperature coefficient, a rise in the junction temperature causes voltage to increase, and therefore current is self-regulated in order to equalize the junction temperature in chips connected in parallel. This characteristic is used to configure stably operating modules.

4.2 Divided DCB substrate

High-power IGBT modules are configured with a maximum of twenty-four IGBT and FWD chips, each, which are connected in a parallel configuration. In order to ensure power cycle capability and to improve mass productivity, a structure is adopted that divides the DCB (direct copper bonding) substrate. By dividing the DCB substrate, thermal interference can be reduced and the quality of each DCB substrate can be checked individually, and as a result, productivity can be increased. Figure 9 shows the internal structure of

Fig.9 Internal structure



a high-power IGBT module.

4.3 Optimization of main terminal structure

The following three factors are important in the design of the main terminal structure.

- (1) Equalization of current balance among DCB substrates
- (2) Reduction of internal inductance
- (3) Suppression of temperature rise due to heat generated at main terminal

These three factors involve complex mutually interacting tradeoff relations, and an optimized design that satisfies the requirements of all three of these factors is indispensable.

- (1) Equalization of current balance

The DCB substrate is divided from the location of the module's main terminal into a portion located directly below the emitter terminal and a portion located directly below the collector terminal, and these must be connected in parallel with the shortest wiring possible. However, the implementation of the shortest possible wiring results in a structure prone to inductance imbalance between DCB substrates, and a large current imbalance will occur during switching (turn-on, turn-off, and reverse recovery). Figure 10 shows the difference of currents flowing to the DCB substrate in the case of an inductance imbalance and in the case of balanced inductance. To balance the inductance,

Fig.10 Measurement of current between DCB substrates

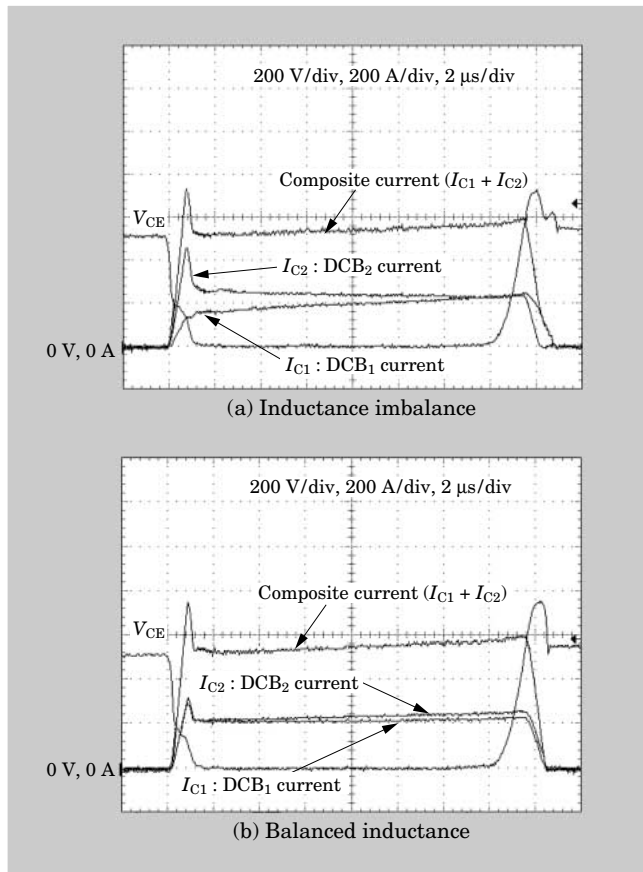
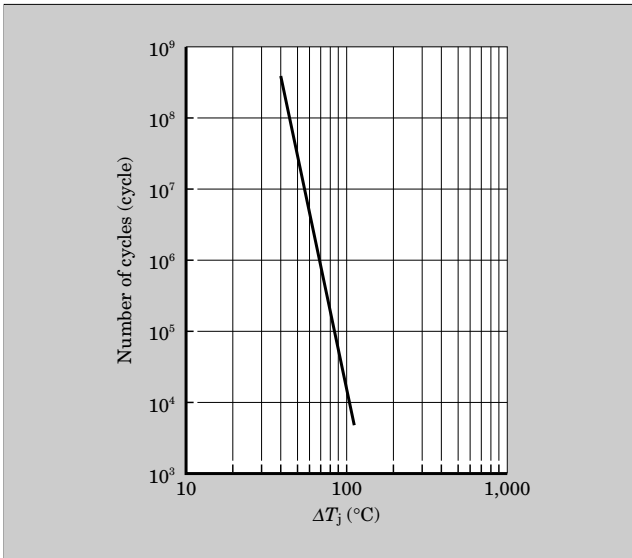


Fig.11 ΔT_j power cycle capability



current pathways inside the emitter terminal and collector terminal were analyzed, and a structure was adopted that balances the current.

(2) Reduction of internal inductance

High-power IGBT modules require the capability to instantaneously turn-off a large current, and it is important to reduce the surge voltage generated inside the package at the event of turn-off. In other words, decreasing the internal inductance of the package becomes an issue. However, the structure described in the above paragraph and introduced to equalize the current balance has the contrary effect of increasing the internal inductance, but by actively utilizing magnetic field interactions, individual inductances can be cancelled and the increase in inductance suppressed. As a result, an extremely small inductance per terminal of approximately 20 nH was realized.

(3) Suppression of temperature rise due to heat generated at main terminal

The main terminal of a high-power IGBT module is required to provide the capability to conduct 1,200 A of current per terminal (single terminal configured from the emitter and collector terminals) in order to configure a 3,600 A (max.) module. The extent to which

temperature rise due to the heat generated by a terminal during current conduction can be suppressed is an issue. By forming the emitter and collector terminals with an outward curvature at their part inside module, the volume of each terminal increases and the temperature rise due to generated heat during current conduction is suppressed.

5. Ensuring the Power Cycle Capability

From the analysis of an IGBT module after power cycle testing, Fuji Electric has verified that the ΔT_j power cycle capability is determined by the combined lifetimes of the under-the-chip solder and the bonding wire. In a high-power IGBT module, by using the higher stiffness material of Sn-Ag as the under-the-chip solder, dividing the DCB substrate to suppress thermal interference, and equalizing current flow among DCB substrates, we verified that the ΔT_j power cycle capability is equal to that of a module having few parallel connections (See Fig. 11). Moreover, we conducted a ΔT_c power cycle test assuming a specific application for high-power IGBT modules in which the case temperature varied widely, and verified the capability to withstand 10,000 cycles at $\Delta T_c = 70^\circ\text{C}$.

6. Conclusion

An overview of Fuji Electric's high-power IGBT module products that use U4-chips has been presented. We are confident that this product group will be able to provide through support of diversified needs. In particular, the reduction in turn-on loss enables a wider range of choices for the gate resistance and improves the ease of use. Fuji Electric remains committed to raising the level of power semiconductor and package technology in order to support additional needs and to developing new products that contribute to the advancement of power electronics.

Reference

- (1) Morozumi, A. et al. Reliability of Power Cycling for IGBT Power Semiconductor Module. Conf. Rec. IEEE Ind. Appl. Conf. 36th. 2001, p.1912-1918.

